International Journal of Hydrogen Energy 172 (2025) 151199

Contents lists available at ScienceDirect

International Journal of Hydrogen Energy

journal homepage: www.elsevier.com/locate/he

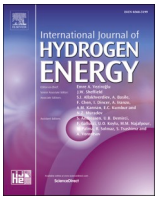

Harmonizing hydrogen nanobubbles with ammonia: molecular perspectives on a novel fuel

Sritay Mistry *, Xinyan Wang

Centre for Advanced Powertrains and Fuels, Brunel University of London, London, UB8 3PH, UK

1. Introduction

The need for new green fuels is well established, driven by efforts for mitigating climate change and building energy security [1,2]. Among green fuels, hydrogen, especially low and zero carbon hydrogen, appears prominent [3]. The UK plans to meet an estimated 20–35 % of its energy needs through hydrogen [3]. Hydrogen as a fuel, however, is not without challenges. Hydrogen adoption faces policy challenges, including creating balanced demand and supply across industries and homes, along with effective pricing. Additionally, there are technological issues with its storage and transportation.

Apart from hydrogen, ammonia also has a sustained interest in the green energy sector. It can be used in fuel cells [4–7], or as a carrier for hydrogen [6,8–11] and as a direct replacement of liquid hydrocarbon fuels [12–17]. Ammonia molecules contain 17.7 % hydrogen atoms by weight, making it an excellent hydrogen carrier [10,11].Interest in ammonia as a fuel in combustion systems is driven by advantages such as an existing large scale distribution infrastructure and a high octane rating of around 120. The major drawbacks of ammonia as a fuel – its low flame speed and long ignition time can be addressed when it is blended with hydrogen [9]. Numerous experimental and numerical studies have therefore been conducted into the flame characteristics, particularly the flame speed and NOx emissions from NH_3/H_2/air combustion [18–21]. Notwithstanding these benefits, blending large quantities of hydrogen with ammonia presents its own challenges. One approach to ammonia-hydrogen fuels is the 'dual fuel' approach, where hydrogen is introduced as a pilot fuel in the combustion chamber alongside ammonia. This approach requires additional hydrogen storage modules, increasing complexity especially in vehicular applications, alongside modifications to engine combustion chamber. A second approach is the direct blend of hydrogen with liquid ammonia, creating a 'monofuel' for its direct use in combustion engines. Bulk hydrogen nanobubbles in liquid ammonia can allow better hydrogen blending. Direct dissolution, by contrast, limits blending to trace amounts [22].

Bulk nanobubbles in liquids are an exciting new field of study, with questions about their existence persisting until recently [23]. Bulk air nanobubbles in water have been observed to last for weeks experimentally [23–25], but there is no universal agreement on the reasons behind their existence and stability. Several theories attempt to explain nanobubble stability. These include free energy changes in the bubble-fluid system, fluid supersaturation, and surface charges on bubbles [26–29].

The pressure within large and nano-bubbles is governed by the well-known Rayleigh-Plesset equation [30], which at steady state simplifies to:

$$P_{gas} + P_{vap.} = P_{bulk} + P_{laplace}, \tag{1}$$

where P_{gas} is the gas pressure inside the bubble, P_{vap} is the pressure of the vapour (from the surrounding liquid) inside the bubble, P_{bulk} is the bulk pressure of the surrounding liquid and $P_{laplace}$ is the Laplace pressure. The Laplace pressure is inversely related to the bubble radius. For large bubbles, this pressure is miniscule, but for micro (R∼10 μ m) and nano-sized (R∼0.1 μ m) bubbles, this pressure varies from 0.01 MPa to 1 MPa, respectively. These high Laplace pressures for nanobubbles led to a belief that it would be impossible for them to exist, and this conjecture is known as the Laplace pressure catastrophe. Contrary to these classical theoretical expectations, bulk nanobubbles have been observed experimentally [23,31–33]. In the absence of well accepted theoretical frameworks, direct numerical simulation methods, such as molecular dynamics (MD) simulations have become a popular tool to complement experimental studies on nanobubbles, especially air/nitrogen nanobubbles in water [34–39]. Fig. 1 demonstrates notable experimental and MD works on nanobubbles.

The experimental confirmation of the existence of bulk nanobubbles raises interesting prospects in their use to enrich both existing [43,49] and new fuels. The high Laplace pressure inside the bubble means that gases can be stored in the form of nanobubbles at a high pressure without the need for pressurized containers. This has obvious advantages when applied to hydrogen nanobubbles in ammonia. Compared to direct blending, enriching liquid ammonia with hydrogen nanobubbles

* Corresponding author.
E-mail address: sritay.mistry@brunel.ac.uk (S. Mistry).

https://doi.org/10.1016/j.ijhydene.2025.151199
Received 12 January 2025; Received in revised form 21 August 2025; Accepted 23 August 2025
Available online 5 September 2025

preserves the high volumetric energy density of ammonia and avoids the logistics of multiple fuels.

Hydrogen nanobubbles is an active area of interest for enhancing fuel characteristics of current carbon-based fuels – with Dr Oh's group investigating the stability and combustion characteristics of hydrogen nanobubble enhanced gasoline [41,43]. They are expected to enhance combustion by creating "micro-explosions", which further atomises the fuel [50]. Recently, Zhang *et .al* [51]. studied the stability and dynamics of hydrogen nanobubbles in water using the MD method, confirming the high Laplace pressures present within and re-iterating the validity of Henry's law at the nanoscales. Bulk hydrogen nanobubbles in ammonia, however, have so far not been observed and studied. It is unknown if hydrogen will form stable nanobubbles in ammonia, and if they do, then what the potential properties of such a fuel mixture will be. In this study, we attempt to establish whether the existing stability theories would be applicable to this particular mixture, and then explore what the energy and fluid properties of such a mixture could be.

The MD works of Weijs et al. [34], followed by the reports by Hong et al. [38] and Gao et al. [47], present a reproducible mechanism of nanobubble stability termed 'diffusive shielding'. This method of stability is observed when dissolved gas concentration around bubbles are high enough to be in equilibrium with the confined, high pressure gas within the bubbles. Other theories of bubble stability, such as those based on zeta potential of bubbles as proposed by Tan et al. [35] are difficult to utilise for this work since surface charges on hydrogen nanobubbles in ammonia, a critical input for these theories, is unknown. Therefore, this work will use the molecular dynamics method alongside a numerical approach using a diffusive model to investigate the stability and properties of hydrogen nanobubbles. This study aligns with experimental work by using parameters like bubble density (bubbles/ml), dissolved gas concentration, bubble radii, and pressure. Atomic-scale parameters are detailed in the electronic supplemetary information (ESI).

2. Methodology

Determining the stability of nanobubbles requires knowledge of the temporal behaviour of the nanobubble, specifically its change in size with time. Nanobubble dynamics are expected to be in the order of a few nanoseconds. They are difficult to be tracked in experimental studies, which can largely report more macroscale parameters such as bubble concentration (usually in bubble/ml), and the size distribution of bubbles at a given instance of time. While numerous theories exist about bubble stability, it is unclear whether it will be applicable to ammonia-hydrogen mixtures, since they are usually framed for air nanobubbles in water, or for simple Lennard-Jones fluids. Molecular dynamics (MD) method is a useful tool in the study of hydrogen nanobubbles in ammonia, specifically to test whether at least one of the theories of stability, through diffusive equilibrium with the surrounding fluid, is applicable to this particular mixture. For this work, MD simulations were carried out using the open-source MD package LAMMPS [52]. Ammonia was simulated using the model proposed by Kristóf et al. [53], due to its accuracy in predicting both the phase-state and the surface tension of ammonia (details in ESI). Hydrogen was modelled using the parameters found in Cheng et al. [54], based on its accurate representation of the gas phase of hydrogen and its low computational cost. The Lorentz-Berthelot (LB) mixing rules were used to characteries the interactions between hydrogen and ammonia molecules. The appropriateness of the LB rules was established by evaluating the Henry constant using the obtained parameters, which were found to be in good agreement with experimental works [22] (details in ESI). The MD simulations used to validate the appropriateness of the selected models is provided in section 1 of the ESI. The temperature of the system was kept constant at 293.15 K using Nóse-Hoover [55] thermostats (i.e., thermal effects on bubble dynamics were neglected). The use of thermostat is unlikely to affect the diffusive processes central to exploring the diffusive stability of the bubble, since the vapour pressures and Henry constant of hydrogen and ammonia were verified with the thermostat applied. Pressure was maintained at 1.2 MPa using a piston on one side of the simulation domain. A piston was used to maintain the pressure to avoid a direct rescaling of the entire simulation domain, as would happen with the use of a barostat, which would also rescale the bubble size. The piston transfers the bulk pressure to the bubble through the liquid, and presents the most realistic way of applying bulk pressure to the entire system. Pistons have been used in other MD studies to apply pressure to both liquid slabs with and without nanobubbles [56–60]. The other, non-piston dimensions were kept periodic. The domain was initialised to a size of $28 \times 28 \times 28$ nm, which for a single bubble, corresponding to a concentration of 4.5×10^{16} bubbles/ml (see Fig. 2). This represents a very high bubble concentration, especially in relation to experimental works depicted in Fig. 1, but is in-line with most MD works. This high concentration also makes the diffusive shielding based stability mechanism easy to study within MD timescales.

A timestep of 0.5 fs was used to allow for the accurate integration of the light hydrogen molecules. The PPPM [61] method was used to calculate long-range electrostatics. Ammonia was equilibrated for 0.1 ns. Hydrogen nanobubbles were then introduced by replacing ammonia molecules in a central spherical region. Hydrogen was added at 5.0 kg/m^3, equating to 6.4 MPa. This hydrogen density was selected for through trial and error, and resulted in a bubble which achieved pressure equilibrium soon after initialisation. Molecules were classified into the gas and liquid phases using Voronoi tessellation [62]. A Voronoi cell

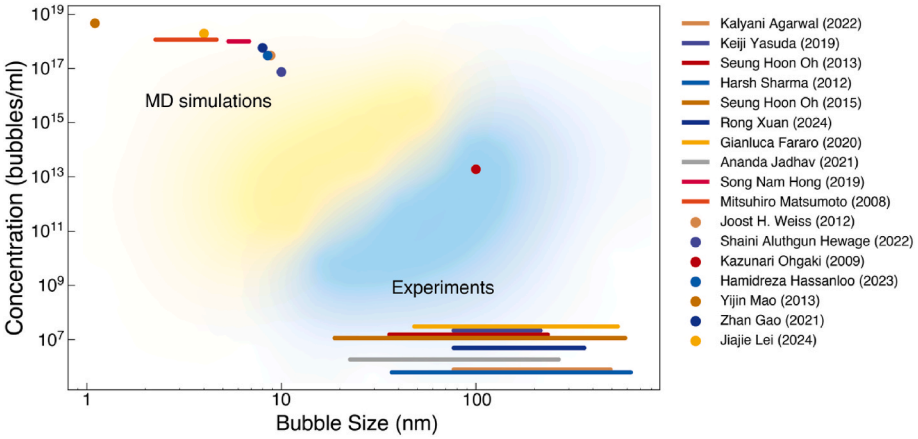

Fig. 1. Bubble sizes and concentration from select MD simulations and experiments. MD struggles to simulate low concentrations (large simulation domains) and large bubble sizes, while experiments struggle to reach high concentrations and low bubble sizes. The literature key refers to Refs. [25,31,33,34,36–48] respectively.

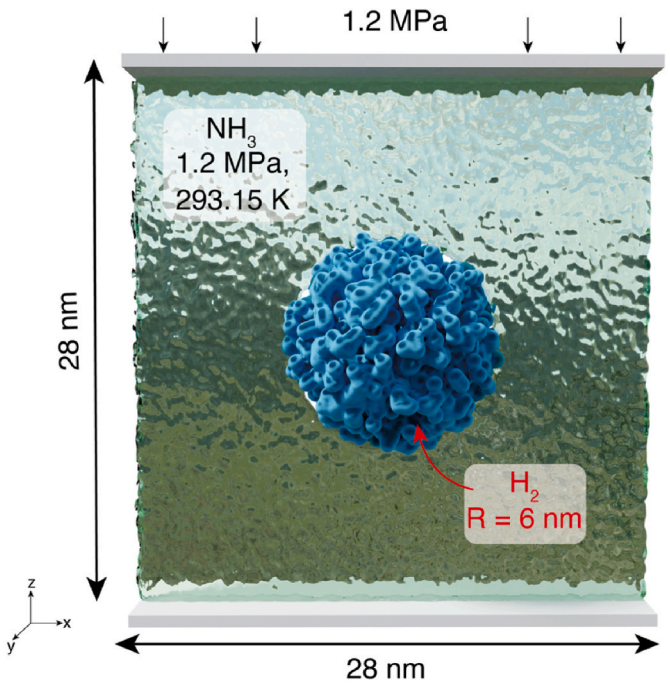

Fig. 2. Setup of MD simulation. Shown here is a R = 6 nm bubble.

volume of 0.105 nm^3, corresponding to a density of 270 kg/m^3 was used as the cutoff value between the liquid and gas phases for ammonia, while a value of 0.07 nm^3, corresponding to 48 kg/m^3 was used for hydrogen. Bubble radius was calculated with the assumption that the bubble occupied a spherical volume, and the bubble volume was calculated using Voronoi tessellation. Theoretical predictions of the bubble dynamics were generated using the Epstein-Plesset equations as given in Epstein et al. [63]. Slight modifications were carried out on the original equation to account for changing dissolved gas quantities in the liquid, using the mass flux equations outlined by the authors. Further details of the modifications are provided in the ESI.

To keep commonality with experimental works, results are provided with bubble concentration as a parameter where possible. MD studies often use the inter-bubble distance instead of the concentration [34,38], however, these two values can be derived from each other with the assumption that a single bubble is simulated in a periodic MD cell. The inter-bubble distance is then equal to the cell size less the bubble diameter, while the concentration is the inverse of the cell volume.

3. Results and discussion

In order to answer the two primary questions - whether a hydrogen nanobubble can be stabilised in liquid ammonia, and the resulting fuel properties of the mixture, this section is divided into two parts. The first part looks into the theoretical underpinnings of the bubble dynamics and its congruence with the observed MD simulations. The second part looks into the fuel properties, primarily the energy density, of such a nanobubble infused fuel.

All simulations and calculations are carried out with the assumption that the temperature is kept constant at 293.15 K, and pressure at 1.2 MPa. These values are chosen such that ammonia and hydrogen can be maintained as a liquid and gas respectively at the given conditions.

3.1. Theoretical framework and bubble dynamics

The growth/collapse dynamics of a gas bubble in a liquid were first formulated by Epstein et al. [63]. Applying the mass diffusion equation to a bubble, an analytical solution for mass diffusion-driven bubble growth/collapse was presented as follows:

$$1-\epsilon^2-2\delta\left[\frac{1}{1-f}-\frac{2}{3}\right](1-\epsilon)+\frac{2\delta^2}{1-f}\left[\frac{1}{1-f}-\frac{2}{3}\right]\ln\left(\frac{\delta+(1-f)}{\delta+(1-f)\epsilon}\right)=\frac{2DH(1-f)}{R_0^2}t, \tag{2}$$

where $\epsilon = \frac{R(t)}{R_0}$, the ratio of the bubble radius R at time t to the initial radius R_0, δ is a constant depending on the surface tension, molecular weight of gas, gas density and temperature, f is the saturation ratio $f = \frac{c_i}{c_s}$, which is the ratio between the initial gas concentration in the fluid (assumed constant during bubble evolution) and the saturated gas concentration, D is the diffusion coefficient of the gas in the liquid (calculations in ESI) and H is the Henry constant, using the same convention as Epstein et al. [63].

Equation (2) assumes the concentration of the dissolved gas, as well as the bulk pressure, does not change during the bubble growth or collapse. This assumption holds when the bubble concentration is very low, such that the gas flux from the collapsing or growing bubble does not change the concentration in the bulk liquid by much. The effect of mass flux into the liquid can be incorporated numerically, by using the relation:

$$\frac{dm}{dt}=4\pi R^2\rho_\infty\frac{dR}{dt}\left\{1+\frac{2\delta R_0}{3R}\right\}, \tag{3}$$

where dm/dt is the mass flux and dR/dt is the bubble interface velocity, to estimate the mass flux of gas into the liquid. Equation (2) can then be used to iteratively solve for the bubble radius with time, with a varying saturation ratio. Details of this approach, henceforth referred to as the 'modified method' can be found in the ESI.

While there are other analytical approaches to bubble stability, such as one outlined by Weijs et al. [34], these set of equations provided by Epstein et al. [63] provide solutions for the temporal evolution of the bubble size alongside diffusive stability in parameters easily applicable to both experiments and simulations, making them the more appropriate choice for our work.

3.2. Bubble collapse and stability

Fig. 3 shows MD simulation results of a small, collapsing hydrogen nanobubble alongside the numerical solutions from Equation (2) alone and our modified approach.

Fig. 3a demonstrates the evolution of a single 6 nm hydrogen nanobubble. The red line denotes the MD result. The dashed blue lines denote the results from Equations (2) and (3). This figure demonstrates the applicability of Epstein et al.'s [63] equations to hydrogen nanobubbles, as a good agreement can be found between them and the MD simulation. Their original equations consider a fixed value of f, while the modifications done in this work (see ESI) incorporates the resulting change in f as the bubble size changes. This modified approach (dark blue line) is a better fit to the bubble size dynamics than the original approach with a fixed f. Fig. 3b further demonstrates the applicability of the original equations of Epstein et al. [63]. as it is able to correctly predict the time taken for bubbles of a range of sizes to collapse. Deviations of the time taken for the bubble to collapse from the $f = 0$ assumption (i.e., no dissolved gases throughout the bubble life) only occur when larger (R > 4 nm) bubbles dissolve significant quantities of gas to the liquid.

Since Fig. 3 has demonstrated the applicability of Epstein's original equations as well as our modified approach to hydrogen nanobubbles in liquid ammonia, we then proceed to examine stability through diffusive shielding using these equations and compare them with our MD simulations of slightly larger bubbles which appear to show stability through such mechanisms. A point to note is that despite the instantaneous non-spherical bubble shapes in the MD simulations, the agreement with Epstein's equations demonstrates that the bubble volume scales as if the

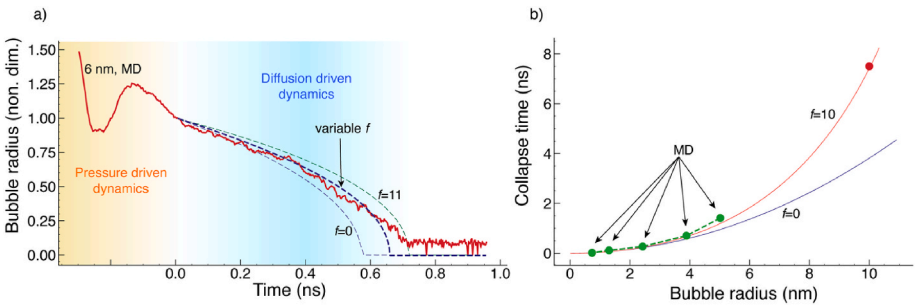

Fig. 3. a) Bubble radius vs time for the 6 nm bubble from MD and theory, the MD trajectory is shifted such that t = 0 and R = 1 after pressure equilibration, b) Bubble collapse time from MD and theory. Different saturation ratios do not affect the collapse time of small bubbles. Red dot indicates predicted collapse time of bubble with R = 10 nm if f = 10. (For interpretation of the references to colour in this figure legend, the reader is referred to the Web version of this article.)

spherical assumption holds true.

The original equation (Equation (2)) does not incorporate a change in f, and is unable to demonstrate stability through diffusive shielding for arbitrary bubble radii and f values, causing the bubble to either grow indefinitely or collapse quickly (red lines in Fig. 4), depending on the f value of the surrounding liquid. Limits of when the bubble transitions from collapse to indefinite growth is given in the ESI.

Stability through diffusive shielding is demonstrated when the effect of mass flux outside the bubble is incorporated through our modified approach, depicted as the blue lines in Fig. 4 (details in ESI). To verify that this diffusive shielding mechanism is applicable to hydrogen nanobubbles in ammonia, results from the original and modified approaches are overlaid with the MD results of a 10 nm bubble in Fig. 5. It is apparent that the bubble in the MD simulation follows the dynamics of the modified approach, demonstrating stability, as against the collapse predicted by Equation (2) in the absence of any dissolved gas. The agreement between the modified approach and MD simulations suggests the applicability of this stability mechanism to the given gas-liquid combination.

The minimum bubble concentration at which a solution with no dissolved gases would have enough gas from dissolving bubbles to make the bubbles dynamically stable varies from 10^{16} bubbles/ml for a 10 nm bubble, to 10^{13} bubbles/ml for a 100 nm bubble. These high concentrations are arrived at when the distance between two bubbles in solution is less than the bubble radius. If bubbles are introduced at a lower concentration, they will collapse due to mass diffusion (given no other stabilisation mechanisms, such as lipid shells or ionic shells). This is consistent with the findings of Weijs et al. [34]. However, subsequent bubble injections into the low or unsaturated solution would keep increasing f till the bubbles become stable and no longer collapse. The absolute dissolved hydrogen concentration needed to stabilise

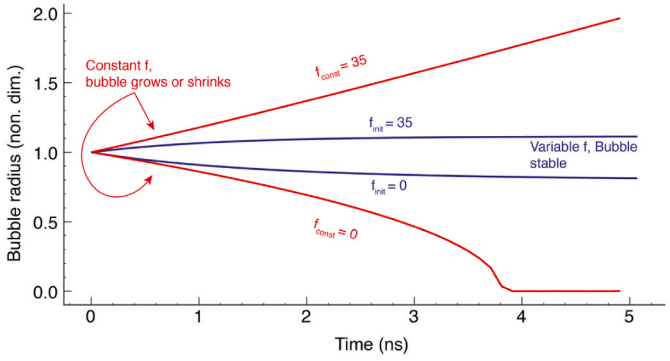

Fig. 4. Bubble evolution with time at constant and various saturation ratios for a 10 nm bubble. Results obtained using equation (2) and the modified approach. For variable f, bubble concentration set to 4.5×10^{16} bubbles/ml, same as in the MD simulations. f_{init} indicates initial concentration ratio with variable f, f_{const} indicates constant f.

nanobubbles in liquid ammonia via diffusive shielding is about the same as in water. At 298 K, the Henry's law constant for hydrogen in water is roughly 3 times greater than in ammonia, indicating that ammonia dissolves significantly more hydrogen at the same partial pressure. However, ammonia's lower surface tension reduces the Laplace pressure, and its high vapour pressure reduces the partial pressure of hydrogen inside a nanobubble, outweighing its higher hydrogen solubility. Consequently, the dissolved gas concentration required for diffusive shielding in ammonia for a 10 nm bubble is theoretically about the same as in water, despite the reduced internal bubble pressure. The relationship between the Henry constant, surface tension and dissolved gas concentration for diffusive stability is described in detail in section 4 of the ESI.

Since stability through diffusive shielding has been demonstrated and verified using two independent methods for hydrogen nanobubbles in ammonia, we proceed to explore the content and properties of such a hypothetical fuel in the next section.

3.3. Fuel properties

This section looks at the fuel properties of the nanobubble mixture, including at the hydrogen and total energy content and the fluid properties of the mixture.

3.3.1. Hydrogen content

Fig. 6 demonstrates the density and pressure of hydrogen within the stable bubbles initialised at $R = 10$ nm at various f values, once they have achieved equilibrium. The density and pressure within the bubble are slightly higher than the expected values given by the Laplace equation, but generally follow the trend of the equation, with smaller bubbles packing hydrogen more densely. This demonstrates that the Laplace equation may be used to predict the hydrogen content of nanobubbles in ammonia. For a 10 nm bubble, the internal pressure is around 8 MPa. A similar sized bubble in water would have an internal pressure of ~30 MPa, following the trend from Zhang et al.

The total amount of hydrogen in the ammonia hydrogen mixture depends on the bubble size, the bubble concentration, and the amount of dissolved hydrogen. Theoretically, the fraction of hydrogen can be maximised by reducing the bubble sizes and increasing the bubble concentration. The limit for bubble concentration is when the inter-bubble distance reduces to zero, i.e., the bubbles touch each other, and no more bubbles can be theoretically accommodated in a given volume. Fig. 7a demonstrates the hydrogen weight fraction variation with the bubble radius, with the assumption that the liquid is super-saturated and the bubble concentration is at the theoretical maximum. The limit of bubble concentration increases with decreasing bubble radius.

Experimental works on nanobubbles have, however, been largely limited to bubble concentrations of $\sim 5 \times 10^8$ bubbles/ml. Furthermore, the liquid is likely to be undersaturated, containing little of the dissolved

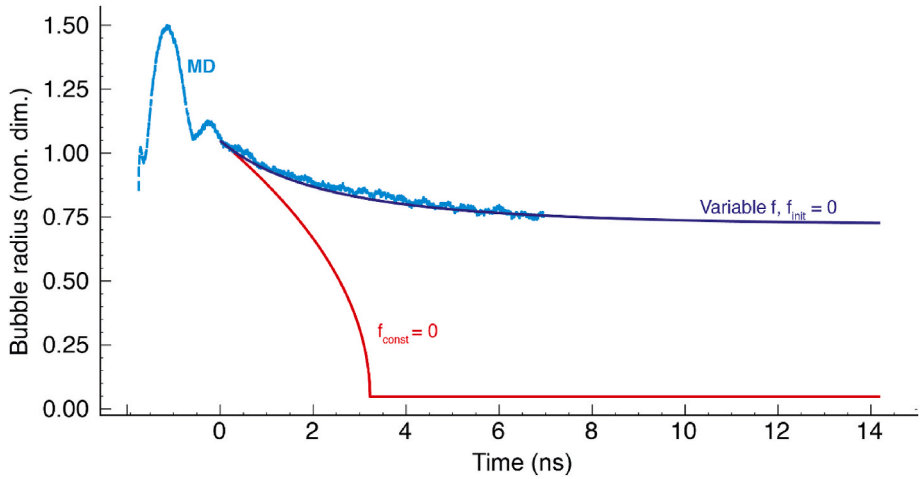

Fig. 5. MD vs theoretical prediction of bubble evolution for an R = 10 nm bubble. For variable f, bubble concentration was set to 4.5×10^{16} bubbles/ml, same as in the MD simulation.

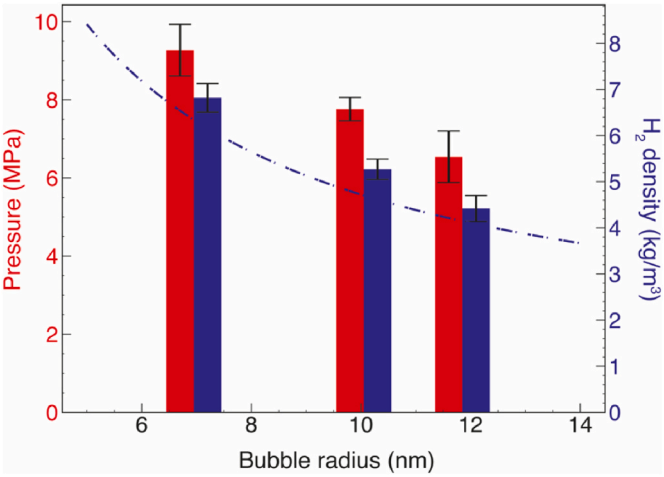

Fig. 6. Hydrogen pressure and density inside bubbles. The dashed line indicates density predicted by the Laplace equation.

gases. Using these two assumptions, Fig. 7b shows increasing hydrogen content with increasing bubble size, assuming no dissolved gases present. The hydrogen content at this bubble concentration is, however, very low, at less than 10^{-8}% by weight. To increase the hydrogen content to substantial amounts, the bubble concentration must be increased, which can be achieved more easily than decreasing the bubble size. In comparison, direct dissolution of hydrogen in liquid ammonia at 1.2 MPa and 293.15 K produces a weight ratio of hydrogen to ammonia of 3.2×10^{-5} or 0.03 g of hydrogen in 1 kg of ammonia. This is two orders of magnitude lower than the weight ratio at maximum concentration for a 1000 nm bubble of about 2×10^{-3}, or 2 g of hydrogen in 1 kg of ammonia.

3.3.2. *Energy density*

Hydrogen has a very high gravimetric energy density, but a low volumetric energy density. Liquid ammonia, in contrast, has high volumetric energy density but a slightly low value of gravimetric energy density, especially when compared to traditional fuels. Infusing hydrogen nanobubbles into ammonia is therefore expected to improve the gravimetric energy density, at a small expense in terms of the volumetric energy density.

The energy density of the nanobubble-ammonia system assumes complete combustion of all fuel components. The lower heating values (LHV) of ammonia and hydrogen are used for all calculations. This is only a theoretical exercise to give some guidance on the expected energy density of ammonia-hydrogen fuel mixtures.

Fig. 8a shows the decrease in volumetric energy density with increasing bubble radius obtained from the MD simulations. The energy density is calculated at the point of bubble initialisation, and where the bubbles are stable in pressure (but not in terms of mass flux). As the bubble diameter increases from 3 to 10 nm, the energy density decreases by 3 %–17 % below that of pure liquid ammonia at 1.2 MPa and 293.15 K. While these decreases are significant, these results are at a fairly high

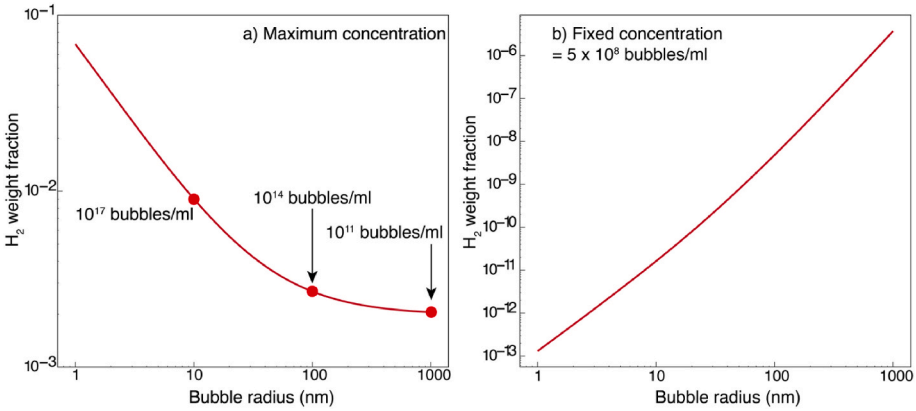

Fig. 7. Variation in hydrogen content with bubble radius at a) maximum concentration and supersaturation b) at fixed concentration.

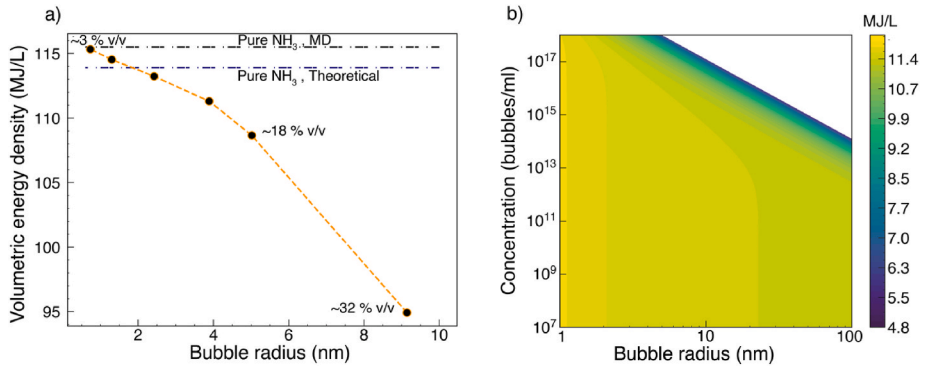

Fig. 8. Volumetric energy density a) From MD simulations, at bubble concentration of 4.5×10^{16} bubbles/ml. b) Contour plot of volumetric energy density variation with bubble size and concentration. The v/v notation denotes the volume ratio of hydrogen to ammonia.

bubble concentration of 4.5×10^{16} bubbles/ml. At more practical concentrations and bubble sizes, Equation S(5) (ESI) is used to calculate the amount of dissolved gas, and therefore arrive at the theoretical values of energy density shown in Fig. 8b over a much wider range of bubble sizes and concentrations. Fig. 8b shows that for most practical nanobubbles with $100\ nm < R < 1000\ nm$ and concentrations below 10^{10} bubbles/ml, the decrease in volumetric energy density is less than 5 %. At the extremes, where the bubbles occupy the theoretical limit of 52.4 % of the total volume, the volumetric energy density drops by a similar 52 %.

Adding hydrogen to ammonia always increases the gravimetric energy density of the resulting mixture because hydrogen gas has high energy and low weight. Fig. 9a shows the linear increase in energy density with increasing bubble size, and therefore, increasing amounts of hydrogen. A 10 nm bubble, at a concentration of 4.5×10^{16} bubbles/ml, provides a ~1 % increase in the gravimetric energy density, at the expense of a ~17 % reduction in the volumetric energy density. Fig. 9b shows the gravimetric energy density using Equation S(5) to calculate the dissolved hydrogen concentration. For most practical cases, i.e., $100\ nm < R < 1000\ nm$ and concentrations below 10^{10} bubbles/ml, the increase in the energy density is <1 %. At the theoretical extreme of concentration where bubbles occupy 52.4 % of the total volume, the gravimetric energy density is increased by ~7 % for a 10 nm bubble, with larger bubbles showing a smaller increase.

Fig. 8b and 9b give a sense of the magnitude of changes expected in the energy density when adding hydrogen nanobubbles to ammonia. Nanobubbles cause a larger drop in the volumetric energy density compared to the increase in the gravimetric energy density. The changes are bound to a ~52 % reduction in volumetric energy density and a 7 % increase in gravimetric energy density at the theoretical upper limit of bubble concentration.

3.3.3. *Fluid properties*

The thermal conductivity, viscosity and surface tension of the stable bubbles at various f ratios was calculated (details in ESI). It is to be noted that properties such as viscosity and thermal conductivity would depend largely on the presence or absence of a bubble within the particular section of interest within the mixture where the properties are being measured. Values measured through MD simulations therefore do not reflect the macroscopic meanings of these values. However, the trends of the values can be reasonably expected to reflect even for macroscopic values. Fig. 10 shows that for all these properties, no significant difference was observed despite the high volume fractions of hydrogen involved. This figure is meant to depict only the direction of change, and not the degree of change. For practical cases, the differences would be insignificant due to much lower bubble concentration, and therefore, a much lower volume fraction. At a concentration of 10^8 bubbles/ml, a typical $R = 100$ nm nanobubble would occupy a volume fraction of 4.2×10^{-9}%, a vanishingly small amount unlikely to influence any fluid properties.

4. Conclusion

This work establishes the theoretical possibility of storing hydrogen nanobubbles in ammonia. While multiple possible pathways to nanobubble stability exist, this work shows the feasibility of stable nanobubbles through the diffusive shielding route for this particular combination of liquid and gas. A high dissolved gas concentration, either through other bubbles or directly dissolved gases, prevents the bubble from either collapsing or growing indefinitely. The hydrogen nanobubbles have a much higher density inside the nanobubble, behaving as a compressed gas without apparent high pressurization of the surrounding fluid. The mixture's energy composition (volumetric and

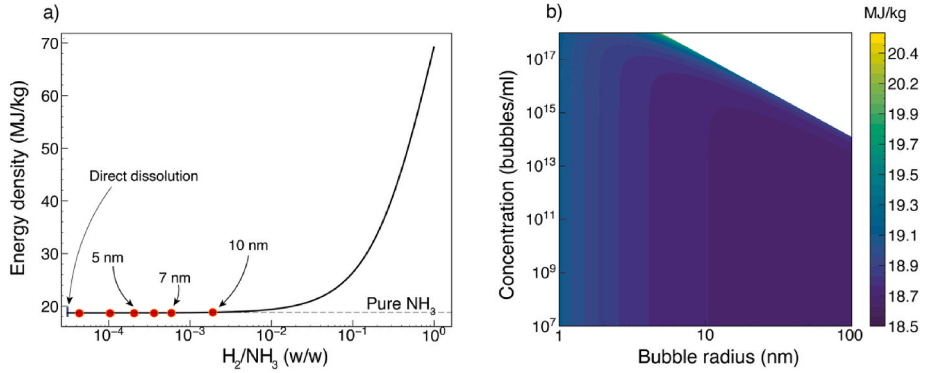

Fig. 9. Gravimetric energy density a) From MD simulations, at bubble concentration of 4.5×10^{16} bubbles/ml. b) Contour plot of gravimetric energy density variation with bubble size and concentration.

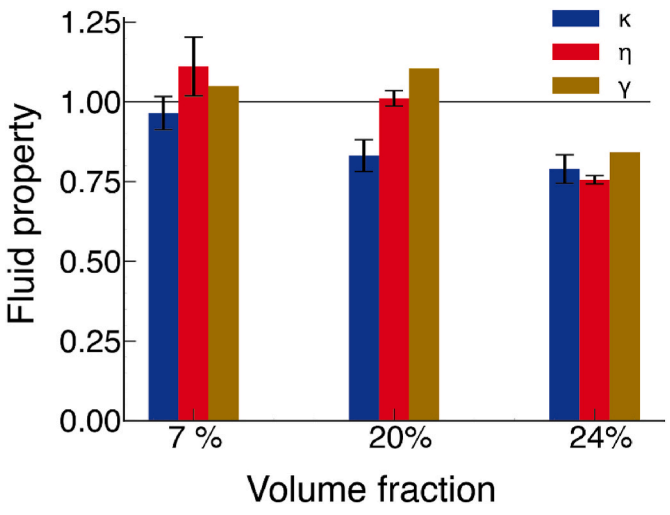

Fig. 10. Thermal conductivity (blue), viscosity (red) and surface tension (chrome) from MD simulations at various hydrogen volume fractions. Values are non-dimensionalised to that of pure ammonia @ 1.2 MPa, 293.15 K. (For interpretation of the references to colour in this figure legend, the reader is referred to the Web version of this article.)

gravimetric density) and fluid properties (thermal conductivity and viscosity) show minimal changes, even at high volume fractions in MD studies.

Further work needs to be done on increasing the concentration of smaller nanobubbles to better realise the benefits of energy storage in nanobubbles. This can potentially be achieved by using surfactants or lipids to generate nanobubble shells, which can protect small nanobubbles from merging together at high concentrations.

CRediT authorship contribution statement

Sritay Mistry: Writing – review & editing, Writing – original draft, Software, Resources, Project administration, Methodology, Investigation, Funding acquisition, Formal analysis. **Xinyan Wang:** Writing – review & editing, Validation, Supervision, Resources, Project administration, Conceptualization.

Declaration of competing interest

The authors declare that they have no known competing financial interests or personal relationships that could have appeared to influence the work reported in this paper.

Acknowledgements

This work was supported by a EPSRC (EP/X001113/1). Dr Xinyan Wang is also supported by UKRI Future Leaders Fellowship (MR/T042915/1). MD simulations were run on ARCHER2, the UK's National Supercomputing Service and MMM Hub Young. The data of this paper can be accessed from the Brunel University London data archive, figshare at https://brunel.figshare.com.

Appendix A. Supplementary data

Supplementary data to this article can be found online at https://doi.org/10.1016/j.ijhydene.2025.151199.

The supplementary information provides additional details supporting the main manuscript:

Figuress. S1-S3 present the ammonia model, slab simulation setup and evolution of the saturation pressure.

Table S1 contrasts ammonia fluid properties to reference values.

Figures. S4-S5 the hydrogen model used and its validation.

Figure S6 demonstrates theoretical limit of saturation ratio for bubble stability.

Figure S7 shows bubble radius evolution with time for various initial radii.

Figure S8 shows MSD calculations for hydrogen.

Figure S9 shows thermal conductivity of pure ammonia using both NEMD and GK methods.

References

[1] Nations, U. Renewable energy – powering a safer future | United Nations.
[2] Great Britain. HM Government. & Great Britain. Department for energy security and net zero. Powering up Britain: Energy Security Plan.
[3] Department for Business E. UK Hydrogen Strategy. 2021. I. S. G. B.
[4] Afif A, et al. Ammonia-fed fuel cells: a comprehensive review. Renew Sustain Energy Rev 2016;60:822–35.
[5] Lan R, Tao S. Ammonia as a suitable fuel for fuel cells. Front Energy Res 2014;2:110206.
[6] Jeerh G, Zhang M, Tao S. Recent progress in ammonia fuel cells and their potential applications. J Mater Chem A Mater 2021;9:727–52.
[7] Valera-Medina A, et al. Review on ammonia as a potential fuel: from synthesis to economics. Energy Fuels 2021;35:6964–7029.
[8] Chehade G, Dincer I. Progress in green ammonia production as potential carbon-free fuel. Fuel 2021;299:120845.
[9] Herbinet O, Bartocci P, Grinberg Dana A. On the use of ammonia as a fuel – a perspective. Fuel Commun 2022;11:100064.
[10] Chiuta S, Everson RC, Neomagus HWJP, Van Der Gryp P, Bessarabov DG. Reactor technology options for distributed hydrogen generation via ammonia decomposition: a review. Int J Hydrogen Energy 2013;38:14968–91.
[11] Zamfirescu C, Dincer I. Ammonia as a green fuel and hydrogen source for vehicular applications. Fuel Process Technol 2009;90:729–37.
[12] Erdemir D, Dincer I. A perspective on the use of ammonia as a clean fuel: challenges and solutions. Int J Energy Res 2021;45:4827–34.
[13] Al-Dawody MF, et al. Mechanical engineering advantages of a dual fuel diesel engine powered by diesel and aqueous ammonia blends. Fuel 2023;346:128398.
[14] Hansson J, Brynolf S, Fridell E, Lehtveer M. The potential role of ammonia as marine fuel—based on energy systems modeling and multi-criteria decision analysis. Sustainability 2020;12:3265. 12, 3265 (2020).
[15] Kim S, Dodds PE, Butnar I. The position of ammonia in decarbonising maritime industry: an overview and perspectives: part I : technological advantages and the momentum towards ammonia-propelled shipping. Johnson Matthey Technol Rev 2021;65:263–74.
[16] Chai WS, Bao Y, Jin P, Tang G, Zhou L. A review on ammonia, ammonia-hydrogen and ammonia-methane fuels. Renew Sustain Energy Rev 2021;147:111254.
[17] Dolan RH, Anderson JE, Wallington TJ. Outlook for ammonia as a sustainable transportation fuel. Sustain Energy Fuels 2021;5:4830–41.
[18] Ichikawa A, et al. Laminar burning velocity and Markstein length of ammonia/hydrogen/air premixed flames at elevated pressures. Int J Hydrogen Energy 2015;40:9570–8.
[19] Kumar P, Meyer TR. Experimental and modeling study of chemical-kinetics mechanisms for H2–NH3–air mixtures in laminar premixed jet flames. Fuel 2013;108:166–76.
[20] Lee JH, Kim JH, Park JH, Kwon OC. Studies on properties of laminar premixed hydrogen-added ammonia/air flames for hydrogen production. Int J Hydrogen Energy 2010;35:1054–64.
[21] Lee JH, Lee SI, Kwon OC. Effects of ammonia substitution on hydrogen/air flame propagation and emissions. Int J Hydrogen Energy 2010;35:11332–41.
[22] Moore RG, Otto FD. The solubility of hydrogen in aliphatic amines. Can J Chem Eng 1972;50:355–60.
[23] Jadhav AJ, Barigou M. Bulk nanobubbles or not nanobubbles: that is the question. Langmuir 2020;36:1699–708.
[24] Ushikubo FY, et al. Evidence of the existence and the stability of nano-bubbles in water. Colloids Surf A Physicochem Eng Asp 2010;361:31–7.
[25] Ohgaki K, Khanh NQ, Joden Y, Tsuji A, Nakagawa T. Physicochemical approach to nanobubble solutions. Chem Eng Sci 2010;65:1296–300.
[26] Manning GS. On the thermodynamic stability of bubbles, immiscible droplets, and cavities. Phys Chem Chem Phys 2020;22:17523–31.
[27] Makkonen L, Vehmas T. Comment on "On the thermodynamic stability of bubbles, immiscible droplets, and cavities"Manning GS, editor. Phys Chem Chem Phys 2020:22. 17523. Physical Chemistry Chemical Physics 23, 12490–12492 (2021).
[28] Vehmas T, Makkonen L. Metastable nanobubbles. ACS Omega 2021;6:8021–7.
[29] Koshoridze SI, Levin YK. Stability of charged nanobubbles in water. Tech Phys Lett 2018;44:1245–7.
[30] Brennen CE. Cavitation and bubble dynamics. Cavitation and bubble dynamics. 2013. p. 1–249. https://doi.org/10.1017/CBO9781107338760.
[31] Agarwal K, Trivedi M, Nirmalkar N. Bulk nanobubbles in aqueous salt solution. Mater Today Proc 2022;57:1789–92.
[32] Nirmalkar N, Pacek AW, Barigou M. On the existence and stability of bulk nanobubbles. Langmuir 2018;34:10964–73.
[33] Jadhav AJ, Ferraro G, Barigou M. Generation of bulk nanobubbles using a high-shear rotor-stator device. Ind Eng Chem Res 2021;60:8597–606.

[34] Weijs JH, Seddon JRT, Lohse D. Diffusive shielding stabilizes bulk nanobubble clusters. ChemPhysChem 2012;13:2197–204.
[35] Tan BH, An H, Ohl CD. How bulk nanobubbles might survive. Phys Rev Lett 2020; 124:134503.
[36] Aluthgun Hewage S, Meegoda JN. Molecular dynamics simulation of bulk nanobubbles. Colloids Surf A Physicochem Eng Asp 2022;650:129565.
[37] Matsumoto M. Surface tension and stability of a nanobubble in water: molecular simulation. J Fluid Sci Technol 2008;3:922–9.
[38] Hong SN, Choe SH, Jong UG, Pak MS, Yu CJ. The maximum interbubble distance in relation to the radius of spherical stable nanobubble in liquid water: a molecular dynamics study. Fluid Phase Equilib 2019;487:45–51.
[39] Hassanloo H, Wang X. Formation, coalescence and behaviour of bulk nanobubbles in dodecane and isooctane and their thermophysical properties: a comprehensive molecular study. Fuel 2024;358:130254.
[40] Yasuda K, Matsushima H, Asakura Y. Generation and reduction of bulk nanobubbles by ultrasonic irradiation. Chem Eng Sci 2019;195:455–61.
[41] Oh SH, Yoon SH, Song H, Han JG, Kim JM. Effect of hydrogen nanobubble addition on combustion characteristics of gasoline engine. Int J Hydrogen Energy 2013;38: 14849–53.
[42] Sharma H, Nirmalkar N. Enhanced gas-liquid mass transfer coefficient by bulk nanobubbles in water. Mater Today Proc 2022;57:1838–41.
[43] Oh SH, Han JG, Kim JM. Long-term stability of hydrogen nanobubble fuel. Fuel 2015;158:399–404.
[44] Xuan R, et al. Study on spray characteristics of micro-nano bubble premixed fuel. Fuel 2024;363:131035.
[45] Ferraro G, Jadhav AJ, Barigou MA. Henry's law method for generating bulk nanobubbles. Nanoscale 2020;12:15869–79.
[46] Mao Y, Zhang Y. Nonequilibrium molecular dynamics simulation of nanobubble growth and annihilation in liquid water. Nanoscale Microscale Thermophys Eng 2013;17:79–91.
[47] Gao Z, Wu W, Sun W, Wang B. Understanding the stabilization of a bulk nanobubble: a molecular dynamics analysis. Langmuir 2021;37:11281–91.
[48] Lei J, Huang D, Zhao W, Liu S, Yue Y. Investigating the stability mechanisms of single bulk nanobubbles: a molecular dynamics perspective. Int J Heat Mass Tran 2024;225:125407.
[49] Kurumanghat V, Sharma H, Nirmalkar N, Kabiraj L. Experimental studies on the effect of bulk nanobubbles on the combustion of Jet A-1. Fuel 2025;398:135385.
[50] Li H, Tian C, Xu X. Fuel oil combustion pollution and hydrogen-water blending technologies for emission mitigation: current advancements and future challenges. Clean Energy Sustain 2025;3:10010. 2025.
[51] Zhang J, et al. Stability and dynamic characteristics of hydrogen nanobubble. Phys Fluids 2025;37.
[52] Thompson AP, et al. LAMMPS - a flexible simulation tool for particle-based materials modeling at the atomic, meso, and continuum scales. Comput Phys Commun 2022;271:108171.
[53] Kristóf T, et al. A simple effective pair potential for the molecular simulation of the thermodynamic properties of ammonia. Mol Phys 1999;97:1129–37.
[54] Cheng H, et al. Molecular dynamics simulations on the effects of diameter and chirality on hydrogen adsorption in single walled carbon nanotubes. J Phys Chem B 2005;109:3780–6.
[55] Nosé S. A unified formulation of the constant temperature molecular dynamics methods. J Chem Phys 1984;81:511–9.
[56] Casanova S, et al. Enhanced nanoparticle rejection in aligned boron nitride nanotube membranes. Nanoscale 2020;12:21138–45.
[57] Dockar D, Borg MK, Reese JM. Mechanical stability of surface nanobubbles. Langmuir 2019;35:9325–33.
[58] Fu Q, et al. Many-body dissipative particle dynamics analysis: generation and stability of bulk nanobubbles under the influence of pressure. J Mol Liq 2024;413: 126005.
[59] Ali Abdol M, Sadeghzadeh S, Jalaly M, Mahdi Khatibi M. On the desalination performance of multi-layer graphene membranes; A molecular dynamics study. Comput Mater Sci 2021;191:110335.
[60] Megha M, John N, Pramada SK, Arunkumar R. Analysis of graphene as a potential filtration membrane for desalination at varying operating conditions using molecular dynamics simulation and response surface methodology. Water Sci Technol 2024;90:1957–70.
[61] Hockney RW, Eastwood JW. Computer simulation using particles. Computer simulation using particles. 1988. https://doi.org/10.1887/0852743920.
[62] Rycroft CH. VORO++: a three-dimensional Voronoi cell library in C++. Chaos 2009;19.
[63] Epstein PS, Plesset MS. On the stability of gas bubbles in liquid-gas solutions. J Chem Phys 2004;18:1505.